

· 研究论文 ·

Synthesis and biological evaluation of noscapine analogues as microtubule-interfering agents

DAI Hou-ling¹, ZHENG Jian-bin^{1*}, LIN Min¹, ZHENG Jing¹, ZHOU Fu-sheng²,
DONG Xiao-chun², GUO Lei¹, LIU Jian-wen¹, WEN Ren^{1,2}

(1. Shanghai Key Laboratory of New Drug Design, School of Pharmacy, East China University of Science and Technology, Shanghai 200237, China; 2. School of Pharmacy, Fudan University, Shanghai 201203, China)

Abstract: A series of noscapine analogues have been synthesized via 13-step reaction starting from 2-hydroxy-3-methoxybenzaldehyde. Anti-tumor activities of these compounds were evaluated against HL-60 cell lines *in vitro* by the standard MTT assay. It was found that most of these derivatives showed appreciable inhibitory activity against HL-60 and tubulin polymerization. The results also indicated that the potency of compound **31** is about three times more than that of noscapine against HL-60 cell line and tubulin polymerization. Moreover, it induced a massive accumulation of cells in G₂/M phase. These results showed noscapine and its derivatives were worth to be intensively studied further.

Key words: noscapine; tubulin; cytotoxic activity; microtubule-interfering agent

CLC number: R916

Document code: A

Article ID: 0513-4870 (2012) 10-1347-11

那可丁衍生物合成及其作为微管干扰药物的生物学评估

戴厚玲¹, 郑剑斌^{1*}, 林敏¹, 郑静¹, 周福生², 董肖椿²,
郭磊¹, 刘建文¹, 闻韧^{1,2}

(1. 华东理工大学药学院, 上海市新药设计重点实验室, 上海 200237; 2. 复旦大学药学院, 上海 201203)

摘要: 以 2-羟基-3-甲氧基苯甲醛为原料, 经 13 步反应合成了 26 个那可丁衍生物。以 HL-60 细胞为靶细胞, 采用 MTT 法进行了初步的体外抗肿瘤活性研究。结果表明, 大多数化合物对 HL-60 细胞株显示出较好的抑制活性和对微管聚合的抑制作用。优选出的化合物 **31** 对 HL-60 细胞株以及微管聚合的抑制活性是那可丁的 3 倍并诱导 HL-60 细胞在 G₂/M 期累积, 这为那可丁及其衍生物的抗肿瘤活性构效关系的研究打下了基础, 值得进一步研究。

关键词: 那可丁; 微管; 细胞毒活性; 微管干扰药物

Microtubule-targeting agents such as the vinca and taxanes alkaloids have been used to treat a wide variety of human cancers. However, the clinical use of these drugs has been hampered by limited effectiveness,

increased drug resistance in tumors, poor bioavailability and side effects including myelosuppression, diarrhea, leucocytopenias, peripheral neuropathies and alopecia^[1,2]. Therefore, there is still an urgent need to search effective drugs possessing favorable toxicity profiles, better therapeutic index and pharmacological characteristics.

α -(-)-Noscapine (**1**, Figure 1), a natural benzyli-soquinoline alkaloid, has been commonly used as an antitussive agent for several decades without significant side effects^[3]. In recent years, noscapine was found to

Received 2012-03-29; Accepted 2012-04-25.

Project supported by the National Science Foundation of China (21102044); Shanghai Committee of Science and Technology (11DZ2260600).

*Corresponding author Tel / Fax: 86-21-64251984,
E-mail: jianbinz@ecust.edu.cn

effectively inhibit a wide variety of cancer types, such as lymphoma, melanoma, breast tumor, ovarian carcinoma and glioblastoma multiforme in animal models without significant toxicity to the animals' vital organs^[4–12].

It has also been identified that noscapine binds to tubulin and alters microtubule dynamics^[4]. Furthermore, noscapine has been in Phase I/II clinical trials for non-Hodgkin's lymphoma or chronic lymphocytic leukemia refractory to chemotherapy^[7]. Due to the efficacy and safety of noscapine as antitumor agent, the efforts had been made to seek more potent analogues of noscapine. Aneja et al^[13] have reported that cyclic ether fluorinated noscapine analogue inhibited proliferation of breast cancer cells including a drug-resistant variant much more potently than noscapine. 9'-Haloderivatives of noscapine was reported as a potential cytotoxic agent against U-87 human glioblastoma cell lines^[1]. Anderson and co-workers have reported that the replacement of 7-methoxyl group of noscapine by amino group (compound **2**, Figure 1) had showed significant enhancement in cytotoxicity against HEK293 cells and microtubule inhibition compared to noscapine^[14].

However, up to now the noscapine studies by chemical modification are still rare. Most of noscapine derivatives were synthesized using natural α -(-)-noscapine as starting material^[13, 14]. In this paper, we introduce the substituted amino or amido group on the 6-position of phthalide ring and discuss the structure-activity relationship (SAR). A series of novel noscapine derivatives were first designed and synthesized, and then their cytotoxicity, cell cycle effects, tubulin binding affinity and inhibition of tubulin polymerization have

been evaluated.

Initially, the synthesis route for starting material aldehydes **6a** and **6b** were prepared from commercially available *o*-vanillin **3** as described in Scheme 1. **3** was converted to pyrogallol 1-monomethyl ether **4** using Dakin oxidation^[15]. Methylation of **4** with CH_2Br_2 afforded **5**, and then treated with POCl_3 and DMF to give a mixture of **6a** and **6b**, which were isolated by flash chromatography.

Compounds **12** and **13** were synthesized by a known methodology^[16] that was modified as depicted in Scheme 2. Aldehyde **6a** was condensed with aminoacetaldehyde dimethyl acetal in toluene, and then were reduced to give **8** with KBH_4 in methanol. Methylation of **8** with formaldehyde and glacial acetic acid, and directly reduced with KBH_4 to provide **9**, which was cyclized to furnish **10** in $6 \text{ mol}\cdot\text{L}^{-1}$ HCl. Reduction of **10** with trifluoroacetic acid and KBH_4 afforded tetrahydroisoquinoline **11**. Isoquinolinium iodide **12** was prepared by reaction of **11** with iodine and potassium acetate. Subsequent treatment of **12** with sodium sulfite in basic solution afforded 1-hydroxyl tetrahydroisoquinoline **13**.

Two stereoisomers of noscapine **16–17** were prepared by bromination of methoxyphthalide **14**, followed by alkylation of 3-bromo-methoxyphthalide **15** with isoquinolinium iodide **12**^[17]. Derivatives **20–21** with electron withdrawing group on phthalide were synthesized from phthalides **18–19** with intermediate **13**. **21** was reduced with hydrated stannous chloride to give the desired aniline **22** (Scheme 3)^[18].

Reaction of aniline **22** with the corresponding

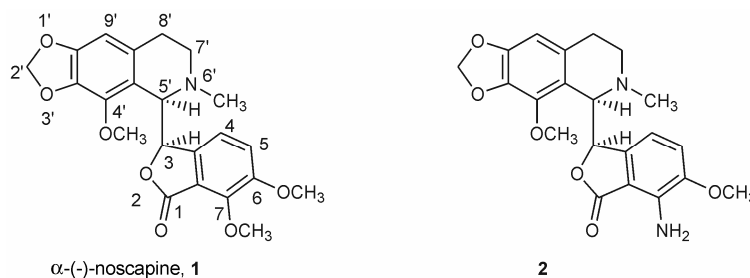
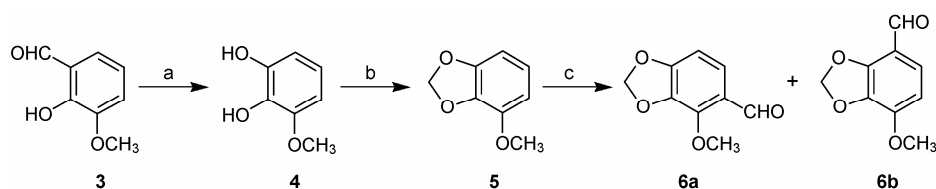
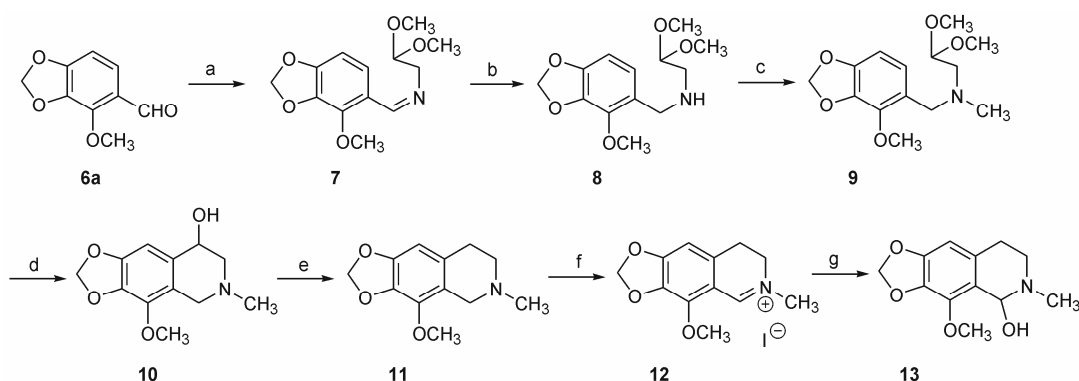


Figure 1 Structures of α -(-)-noscapine **1** and compound **2**



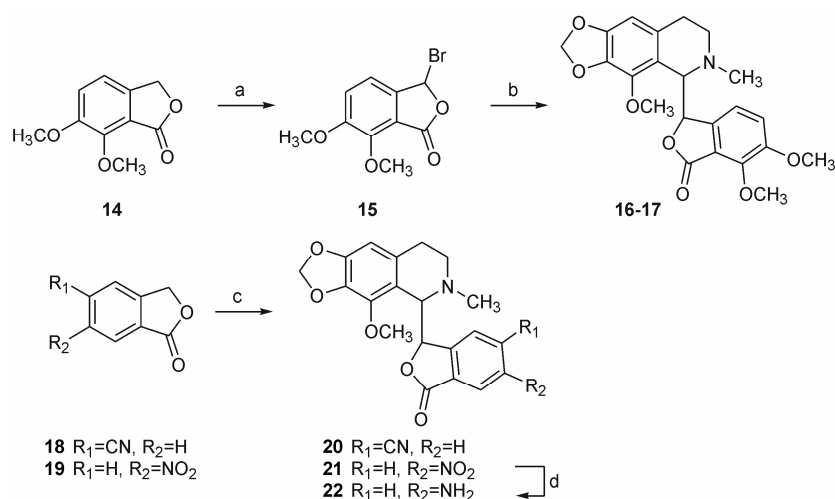
Reagents and conditions: (a) $2 \text{ mol}\cdot\text{L}^{-1}$ NaOH, 6% H_2O_2 , 40–50 °C; (b) CH_2Br_2 , CuO, K_2CO_3 , DMF, reflux; (c) POCl_3 , DMF, 50→90 °C

Scheme 1 The synthesis of compounds **6a** and **6b**



Reagents and conditions: (a) $\text{NH}_2\text{CH}_2\text{CH}(\text{OCH}_3)_2$, toluene, reflux; (b) NaBH_4 , CH_3OH , r.t.; (c) 37% HCHO , HOAc , KBH_4 , CH_3CN , 0–5 °C; (d) $6 \text{ mol}\cdot\text{L}^{-1}$ HCl , r.t.; (e) TFA , KBH_4 , CH_2Cl_2 , 0 °C → r.t.; (f) KOAc , I_2 , EtOH , reflux; (g) Na_2SO_3 , H_2O , 25% NaOH , 40 °C

Scheme 2 The synthesis of compounds **12** and **13**

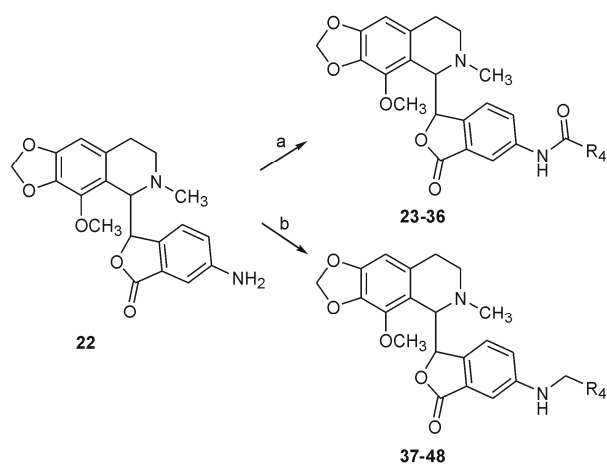


Reagents and conditions: (a) NBS , CCl_4 , reflux; (b) **12**, Zn , CH_3CN , r.t.; (c) **13**, ethanol, reflux; (d) $\text{SnCl}_2\cdot 2\text{H}_2\text{O}$, Sn , HOAc , r.t.

Scheme 3 The synthesis of compounds **16–21**

acid anhydride or acyl chlorides in the presence of a catalytic amount of pyridine gave 6-amido substituted derivatives **23–36**. Reductive amination of **22** with aldehydes in the presence of sodium triacetoxyborohydride and potassium borohydride furnished 6-alkylamino substituted derivatives **37–48** (Scheme 4). The final products were purified by silica gel column chromatography. The configurations were determined by chromatographic and spectroscopic comparison with data in previous references^[17–19]. The H-4 signal in the ^1H NMR spectrum of amine **22** was found relatively upfield at 6.13 ppm. The value was compared with the corresponding chemical shift for α -noscapine, which is 6.16 ppm due to a twist half-chair of piperidine ring (in β -noscapine, this value is 7.25 ppm). Moreover, the N- CH_3 signal of amine **22** was found relatively upfield at 2.41 ppm. The value was compared with the corresponding chemical shift for α -noscapine, which is 2.43 ppm (in β -noscapine, this value is 2.04 ppm).

Therefore, the configurations of compounds **23–48** have been assigned as *erythro* isomers by the comparison



Reagents and conditions: (a) R_4COCl or $(\text{R}_4\text{CO})_2\text{O}$; (b) (1) R_4CHO , HOAc , $\text{NaBH}(\text{OAc})_3$, (2) KBH_4 , CH_3OH (for R_4 see Table 3)

Scheme 4 The synthesis of compounds **23–48**

of the chemical shifts of H-4 and N-CH₃ of the molecules.

Results and discussion

1 Physicochemical properties of noscapine analogues

The physicochemical properties of compounds **23**–**48** were shown in Table 1.

2 The biological evaluation of noscapine analogues

The target compounds were evaluated for their cytotoxic activities using a MTT assay against human acute promyelocytic leukemia cell line HL-60^[20]. The IC₅₀ values of MTT assay for compounds **16**–**17** and **20**–**22** were shown in Table 2. In general, the racemic mixture of noscapine derivatives were less potent than natural noscapine **1**. *Erythro* isomers with the same configuration to natural products shown more active

cytotoxicity against HL-60 compared with their *threo* isomers, which may suggest the importance of the configuration in noscapine. The compound with amino group exhibited more activity than natural noscapine. So, the most potent cytotoxic compound **22** was further modified with substituent amido and amino on the phthalide.

The IC₅₀ values of MTT assay for derivatives **23**–**48** were presented in Table 3. Among the twenty-six compounds, ten compounds showed appreciable cytotoxic activities with IC₅₀ < 20 μmol·L⁻¹ against HL-60 cell line. The most active compounds was 6-amido derivative **31** (IC₅₀ = 6.74 μmol·L⁻¹), which had IC₅₀ three times less than α(-)-noscapine (IC₅₀ = 19.72 μmol·L⁻¹) and equivalent to colchicine (IC₅₀ = 7.45 μmol·L⁻¹).

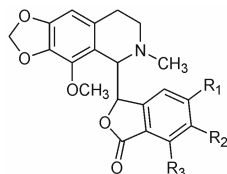
Compound **31**, possessing a nitro group at *para*

Table 1 Physicochemical properties of noscapine derivatives (**23**–**48**)

No.	Property& yield	mp/°C	¹ H NMR (DMSO- <i>d</i> ₆)	MS
23	White powder, 17.4%	266–267	1.84–2.59 (4H, m, CH ₂ CH ₂), 2.45 (3H, s, NCH ₃), 3.98 (3H, s, OCH ₃), 4.31 (1H, d, <i>J</i> = 4 Hz, CH-N), 5.69 (1H, d, <i>J</i> = 4 Hz, CH-O), 6.02 (2H, s, OCH ₂ O), 6.50 (1H, s, Ar-H), 6.51 (1H, d, <i>J</i> = 8 Hz, Ar-H), 7.55 (2H, m, Ar-H), 7.62 (1H, t, Ar-H), 7.86 (1H, dd, <i>J</i> = 2, 8 Hz, Ar-H), 7.96 (2H, d, Ar-H), 8.29 (1H, d, Ar-H), 10.53 (1H, s, CONH)	MALDI-FTMS calcd. For C ₂₇ H ₂₅ N ₂ O ₆ : [M+H] ⁺ 473.171 2. Found 473.170 7
24	Yellow powder, 50.3%	250–251	1.82–2.59 (4H, m, CH ₂ H ₂), 2.45 (3H, s, NCH ₃), 3.98 (3H, s, OCH ₃), 4.31 (1H, d, <i>J</i> = 4 Hz, CH-N), 5.69 (1H, d, <i>J</i> = 4 Hz, CH-O), 6.02 (2H, d, OCH ₂ O), 6.51 (2H, m, Ar-H), 7.39 (2H, m, Ar-H), 7.84 (1H, dd, Ar-H), 8.05 (2H, m, Ar-H), 8.27 (1H, d, Ar-H), 10.54 (1H, s, CONH)	MALDI-FTMS calcd. For C ₂₇ H ₂₄ N ₂ O ₆ F: [M+H] ⁺ 491.161 3. Found 491.161 3
25	Yellow powder, 11.2%	247–248	1.83–2.56 (4H, m, CH ₂ CH ₂), 2.45 (3H, s, NCH ₃), 3.99 (3H, s, OCH ₃), 4.31 (1H, d, <i>J</i> = 4 Hz, CH-N), 5.69 (1H, d, <i>J</i> = 4 Hz, CH-O), 6.02 (2H, s, OCH ₂ O), 6.49 (2H, m, Ar-H), 7.48 (1H, m, Ar-H), 7.54 (1H, m, Ar-H), 7.60 (1H, m, Ar-H), 7.64 (1H, m, Ar-H), 7.74 (1H, m, Ar-H), 8.26 (1H, d, Ar-H), 10.83 (1H, s, CONH)	MALDI-FTMS calcd. For C ₂₇ H ₂₄ N ₂ O ₆ Cl: [M+H] ⁺ 507.132 2. Found 507.131 7
26	Yellow powder, 9.2%	258–260	1.84–2.59 (4H, m, CH ₂ CH ₂), 2.45 (3H, s, NCH ₃), 3.99 (3H, s, OCH ₃), 4.31 (1H, d, <i>J</i> = 4 Hz, CH-N), 5.69 (1H, d, <i>J</i> = 4 Hz, CH-O), 6.02 (2H, s, OCH ₂ O), 6.49 (2H, m, Ar-H), 7.45 (1H, m, Ar-H), 7.52 (1H, m, Ar-H), 7.59 (1H, m, Ar-H), 7.73 (2H, m, Ar-H), 8.26 (1H, d, Ar-H), 10.81 (1H, s, CONH)	MALDI-FTMS calcd. For C ₂₇ H ₂₄ N ₂ O ₆ Br: [M+H] ⁺ 551.080 9. Found 551.081 2
27	Yellow powder, 61.3%	229–231	1.84–2.58 (4H, m, CH ₂ CH ₂), 2.45 (3H, s, NCH ₃), 3.98 (3H, s, OCH ₃), 4.31 (1H, d, <i>J</i> = 4 Hz, CH-N), 5.69 (1H, d, <i>J</i> = 4 Hz, CH-O), 6.02 (2H, s, OCH ₂ O), 6.50 (1H, s, Ar-H), 6.52 (1H, d, <i>J</i> = 8 Hz, Ar-H), 7.53 (1H, t, Ar-H), 7.84 (2H, t, Ar-H), 7.96 (1H, d, <i>J</i> = 8 Hz, Ar-H), 8.16 (1H, t, <i>J</i> = 2 Hz, Ar-H), 8.27 (1H, d, <i>J</i> = 2 Hz, Ar-H), 10.62 (1H, s, CONH)	MALDI-FTMS calcd. For C ₂₇ H ₂₄ N ₂ O ₆ Br: [M+H] ⁺ 551.080 6. Found 551.081 2
28	White powder, 24.4%	258–259	1.87–2.60 (4H, m, CH ₂ CH ₂), 2.45 (3H, s, NCH ₃), 3.85 (3H, s, OCH ₃), 3.98 (3H, s, OCH ₃), 4.31 (1H, brs, CH-N), 5.69 (1H, brs, CH-O), 6.02 (2H, s, OCH ₂ O), 6.50 (2H, m, Ar-H), 7.08 (2H, d, Ar-H), 7.85 (1H, d, Ar-H), 7.97 (2H, d, Ar-H), 8.28 (1H, s, Ar-H), 10.38 (1H, s, CONH)	MALDI-FTMS calcd. For C ₂₈ H ₂₇ N ₂ O ₇ : [M+H] ⁺ 503.182 0. Found 503.181 3
29	White powder, 41.4%	223–225	1.80–2.58 (4H, m, CH ₂ CH ₂), 2.45 (3H, s, NCH ₃), 3.80 (3H, s, OCH ₃), 3.86 (3H, s, OCH ₃), 3.99 (3H, s, OCH ₃), 4.31 (1H, d, <i>J</i> = 4 Hz, CH-N), 5.68 (1H, d, <i>J</i> = 4 Hz, CH-O), 6.02 (2H, s, OCH ₂ O), 6.47 (1H, d, <i>J</i> = 8 Hz, Ar-H), 6.50 (1H, s, Ar-H), 7.11 (1H, m, Ar-H), 7.19 (1H, t, <i>J</i> = 8 Hz, Ar-H), 7.22 (1H, m, Ar-H), 7.75 (1H, dd, <i>J</i> = 8, 1.6 Hz, Ar-H), 8.27 (1H, d, <i>J</i> = 1.6 Hz, Ar-H), 10.57 (1H, s, CONH)	MALDI-FTMS calcd. For C ₂₉ H ₂₉ N ₂ O ₈ : [M+H] ⁺ 533.192 1. Found 533.191 8
30	White powder, 28.3%	224–226	1.79–2.56 (4H, m, CH ₂ CH ₂), 2.45 (3H, s, NCH ₃), 3.97 (3H, s, OCH ₃), 4.31 (1H, d, CH-N), 5.24 (2H, s, CH ₂ O), 5.67 (1H, d, CH-O), 6.03 (2H, s, OCH ₂ O), 6.41 (1H, d, <i>J</i> = 8 Hz, Ar-H), 6.52 (1H, s, Ar-H), 7.11 (1H, t, Ar-H), 7.33 (4H, m, Ar-H), 7.54 (4H, m, Ar-H), 7.66 (1H, dd, Ar-H), 8.21 (1H, s, Ar-H), 10.48 (1H, s, CONH)	MALDI-FTMS calcd. For C ₃₄ H ₃₁ N ₂ O ₇ : [M+H] ⁺ 579.212 4. Found 579.212 6
31	Yellow powder, 87.3%	229–231	1.86–2.62 (4H, m, CH ₂ CH ₂), 2.47 (3H, s, NCH ₃), 3.97 (3H, s, OCH ₃), 4.34 (1H, brs, CH-N), 5.72 (1H, brs, CH-O), 6.01 (2H, s, OCH ₂ O), 6.52 (1H, s, Ar-H), 8.20 (3H, m, Ar-H), 8.29 (1H, s, Ar-H), 8.37 (3H, m, Ar-H), 10.89 (1H, s, CONH)	MALDI-FTMS calcd. For C ₂₇ H ₂₄ N ₃ O ₈ : [M+H] ⁺ 518.157 1. Found 518.155 8
32	Yellow powder, 35.4%	242–243	1.85–2.58 (4H, m, CH ₂ CH ₂), 2.45 (3H, s, NCH ₃), 3.97 (3H, s, OCH ₃), 4.31 (1H, d, <i>J</i> = 4 Hz, CH-N), 5.68 (1H, d, <i>J</i> = 4 Hz, CH-O), 6.02 (2H, s, OCH ₂ O), 6.50 (2H, m, Ar-H), 6.73 (1H, m, Ar-H), 7.37 (1H, d, <i>J</i> = 4 Hz, Ar-H), 7.84 (1H, m, Ar-H), 7.97 (1H, m, Ar-H), 8.26 (1H, m, Ar-H), 10.49 (1H, s, CONH)	MALDI-FTMS calcd. For C ₂₅ H ₂₃ N ₂ O ₇ : [M+H] ⁺ 463.150 6. Found 463.150 0

			Continued	
No.	Property& yield	mp/°C	¹ H NMR (DMSO- <i>d</i> ₆)	MS
33	Yellow powder, 13.5%	203–206	1.85–2.56 (4H, m, CH ₂ CH ₂), 2.45 (3H, s, NCH ₃), 3.98 (3H, s, OCH ₃), 4.32 (1H, brs, CH-N), 5.71 (1H, brs, CH-O), 6.02 (2H, s, OCH ₂ O), 6.52 (2H, m, Ar-H), 7.59 (1H, m, Ar-H), 7.85 (1H, m, Ar-H), 8.29 (2H, m, Ar-H), 8.78 (1H, d, Ar-H), 9.12 (1H, s, Ar-H), 10.73 (1H, s, CONH)	MALDI-FTMS calcd. For C ₂₆ H ₂₄ N ₃ O ₆ : [M+H] ⁺ 474.166 7. Found 474.165 9
34	Yellow powder, 32.1%	202–204	1.90–2.58 (4H, m, CH ₂ CH ₂), 2.51 (3H, s, NCH ₃), 3.97 (3H, s, OCH ₃), 4.33 (1H, brs, CH-N), 5.70 (1H, brs, CH-O), 6.01 (2H, d, OCH ₂ O), 6.51 (2H, s, Ar-H), 7.18 (2H, m, Ar-H), 7.48 (1H, d, Ar-H), 7.87 (1H, brs, Ar-H), 8.19 (1H, d, Ar-H), 8.32 (2H, m, Ar-H), 10.04 (1H, s, NH), 11.81 (1H, s, NH)	MALDI-FTMS calcd. For C ₂₉ H ₂₆ N ₃ O ₆ : [M+H] ⁺ 512.183 4. Found 512.181 6
35	Yellow powder, 30.3%	230–233	1.80–2.58 (4H, m, CH ₂ CH ₂), 2.43 (3H, s, NCH ₃), 2.71 (2H, t, CH ₂), 3.03 (2H, t, CH ₂), 3.96 (3H, s, OCH ₃), 4.29 (1H, s, CH-N), 5.65 (1H, s, CH-O), 6.01 (2H, s, OCH ₂ O), 6.43 (1H, d, <i>J</i> = 8 Hz, Ar-H), 6.48 (1H, s, Ar-H), 6.97 (1H, t, <i>J</i> = 7.2 Hz, Ar-H), 7.06 (1H, t, <i>J</i> = 7.2 Hz, Ar-H), 7.13 (1H, d, Ar-H), 7.32 (1H, d, <i>J</i> = 8 Hz, Ar-H), 7.56 (2H, m, Ar-H), 8.18 (1H, s, Ar-H), 10.25 (1H, s, NH), 10.78 (1H, s, NH)	MALDI-FTMS calcd. For C ₃₁ H ₃₀ N ₃ O ₆ : [M+H] ⁺ 540.214 2. Found 540.212 9
36	White powder, 98.7%	252–253	1.79–2.56 (4H, m, CH ₂ CH ₂), 2.07 (3H, s, CH ₃ CO), 2.43 (3H, s, NCH ₃), 3.96 (3H, s, OCH ₃), 4.28 (1H, d, <i>J</i> = 4 Hz, CH-N), 5.65 (1H, d, <i>J</i> = 4 Hz, CH-O), 6.01 (2H, s, OCH ₂ O), 6.44 (1H, d, <i>J</i> = 8 Hz, Ar-H), 6.48 (1H, s, Ar-H), 7.56 (1H, dd, <i>J</i> = 8, 1.6 Hz, Ar-H), 8.14 (1H, d, <i>J</i> = 1.6 Hz, Ar-H), 10.24 (1H, s, CONH)	(EI) <i>m/z</i> [M] ⁺ 410
37	White powder, 50.2%	187–188	1.94–2.67 (4H, m, CH ₂ CH ₂), 2.54 (3H, s, NCH ₃), 4.03 (3H, s, OCH ₃), 4.21 (1H, s, NH), 4.33 (2H, s, CH ₂ N), 4.41 (1H, d, <i>J</i> = 4 Hz, CH-N), 5.60 (1H, d, <i>J</i> = 4 Hz, CH-O), 5.93 (2H, s, OCH ₂ O), 6.21 (1H, d, <i>J</i> = 8 Hz, Ar-H), 6.31 (1H, s, Ar-H), 6.66 (1H, dd, <i>J</i> = 8, 4 Hz, Ar-H), 7.03 (1H, d, Ar-H), 7.30 (1H, m, Ar-H), 7.34 (4H, d, Ar-H)	MALDI-FTMS calcd. For C ₂₇ H ₂₇ N ₂ O ₅ : [M+H] ⁺ 459.191 3. Found 459.191 4
38	White powder, 94.3%	193–194	1.85–2.65 (4H, m, CH ₂ CH ₂), 2.48 (3H, s, NCH ₃), 3.74 (3H, s, OCH ₃), 3.95 (3H, s, OCH ₃), 4.05 (1H, m, NH), 4.18 (2H, s, CH ₂ NH), 4.34 (1H, d, CH-N), 5.55 (1H, d, CH-O), 5.86 (2H, s, OCH ₂ O), 6.15 (1H, d, Ar-H), 6.24 (1H, s, Ar-H), 6.59 (1H, dd, Ar-H), 6.81 (2H, d, Ar-H), 6.95 (1H, d, Ar-H), 7.20 (2H, d, Ar-H)	MALDI-FTMS calcd. For C ₂₈ H ₂₉ N ₂ O ₆ : [M+H] ⁺ 489.203 0. Found 489.202 0
39	White powder, 14.7%	79–81	1.97–2.65 (4H, m, CH ₂ CH ₂), 2.54 (3H, s, NCH ₃), 2.94 (6H, s, OCH ₃), 4.03 (3H, s, OCH ₃), 4.06 (1H, brs, NH), 4.19 (2H, brs, CH ₂ N), 4.39 (1H, d, <i>J</i> = 4 Hz, CH-N), 5.60 (1H, d, <i>J</i> = 4 Hz, CH-O), 5.93 (2H, s, OCH ₂ O), 6.21 (1H, d, <i>J</i> = 8 Hz, Ar-H), 6.31 (1H, s, Ar-H), 6.65 (1H, dd, <i>J</i> = 8, 2 Hz, Ar-H), 6.71 (2H, d, <i>J</i> = 8.8 Hz, Ar-H), 7.03 (1H, d, <i>J</i> = 2 Hz, Ar-H), 7.22 (2H, d, <i>J</i> = 8.8 Hz, Ar-H)	MALDI-FTMS calcd. For C ₂₉ H ₃₂ N ₃ O ₅ : [M+H] ⁺ 502.234 3. Found 502.233 6
40	White powder, 60.1%	155–158	1.90–2.70 (4H, m, CH ₂ CH ₂), 2.55 (3H, s, NCH ₃), 4.03 (3H, s, OCH ₃), 4.23 (1H, s, NH), 4.31 (2H, s, CH ₂ NH), 4.41 (1H, d, CH-N), 5.62 (1H, d, CH-O), 5.94 (2H, s, OCH ₂ O), 6.22 (1H, d, Ar-H), 6.31 (1H, s, Ar-H), 6.65 (1H, dd, Ar-H), 6.99 (1H, d, Ar-H), 7.23 (2H, d, Ar-H), 7.47 (2H, d, Ar-H)	MALDI-FTMS calcd. For C ₂₇ H ₂₆ N ₂ O ₅ Br: [M+H] ⁺ 537.103 4. Found 537.102 0
41	Yellow powder, 29.3%	113–115	2.00–2.85 (4H, m, CH ₂ CH ₂), 2.60 (3H, s, NCH ₃), 3.86 (3H, s, OCH ₃), 4.49 (4H, m, NH, CH ₂ N and CH-N), 5.77 (1H, d, CH-O), 5.91 (2H, s, OCH ₂ O), 6.30 (1H, s, Ar-H), 6.76 (1H, m, Ar-H), 6.87 (1H, s, Ar-H), 7.26 (1H, s, Ar-H), 7.50 (2H, d, Ar-H), 8.19 (2H, d, Ar-H)	MALDI-FTMS calcd. For C ₂₇ H ₂₆ N ₃ O ₇ : [M+H] ⁺ 504.175 1. Found 504.176 5
42	White powder, 51.3%	159–160	1.93–2.65 (4H, m, CH ₂ CH ₂), 2.54 (3H, s, NCH ₃), 4.03 (3H, s, OCH ₃), 4.17 (1H, m, NH), 4.23 (2H, d, CH ₂ N), 4.40 (1H, d, <i>J</i> = 4 Hz, CH-N), 5.60 (1H, d, <i>J</i> = 4 Hz, CH-O), 5.93 (2H, s, OCH ₂ O), 5.94 (2H, s, OCH ₂ O), 6.21 (1H, d, <i>J</i> = 8 Hz, Ar-H), 6.31 (1H, s, Ar-H), 6.65 (1H, dd, <i>J</i> = 8, 2 Hz, Ar-H), 6.79 (3H, m, Ar-H), 7.00 (1H, brs, Ar-H)	MALDI-FTMS calcd. For C ₂₈ H ₂₇ N ₂ O ₇ : [M+H] ⁺ 503.181 8. Found 503.181 3
43	White powder, 55.3%	202–203	1.98–2.65 (4H, m, CH ₂ CH ₂), 2.54 (3H, s, NCH ₃), 4.02 (3H, s, CH ₃), 4.03 (3H, s, CH ₃), 4.23 (3H, brs, NH and CH ₂ NH), 4.39 (1H, d, <i>J</i> = 4 Hz, CH-N), 5.59 (1H, d, <i>J</i> = 4 Hz, CH-O), 5.93 (4H, s, OCH ₂ O), 6.21 (1H, d, <i>J</i> = 8 Hz, Ar-H), 6.31 (1H, s, Ar-H), 6.46 (1H, d, <i>J</i> = 8 Hz, Ar-H), 6.67 (1H, d, <i>J</i> = 8 Hz, Ar-H), 6.73 (1H, d, <i>J</i> = 8 Hz, Ar-H), 7.03 (1H, s, Ar-H)	MALDI-FTMS calcd. For C ₂₉ H ₂₉ N ₂ O ₈ : [M+H] ⁺ 533.192 4. Found 533.191 8
44	White powder, 39.1%	199–202	1.97–2.65 (4H, m, CH ₂ CH ₂), 2.54 (3H, s, NCH ₃), 3.79 (3H, s, OCH ₃), 3.83 (3H, s, OCH ₃), 4.01 (3H, s, OCH ₃), 4.25 (3H, brs, NH and CH ₂ NH), 4.40 (1H, d, CH-N), 5.59 (1H, d, CH-O), 5.93 (2H, s, OCH ₂ O), 6.21 (1H, d, Ar-H), 6.30 (1H, s, Ar-H), 6.42 (1H, dd, Ar-H), 6.47 (1H, d, Ar-H), 6.67 (1H, dd, Ar-H), 7.04 (1H, d, Ar-H), 7.16 (1H, d, Ar-H)	MALDI-FTMS calcd. For C ₂₉ H ₃₁ N ₂ O ₇ : [M+H] ⁺ 519.213 7. Found 519.212 6
45	Yellow powder, 7.3%	90–93	1.94–2.64 (4H, m, CH ₂ CH ₂), 2.55 (3H, s, NCH ₃), 4.04 (3H, s, OCH ₃), 4.42 (2H, m, CH ₂ N), 4.50 (2H, m, NH and CH-N), 5.63 (1H, d, CH-O), 5.94 (2H, s, OCH ₂ O), 6.24 (1H, d, <i>J</i> = 8 Hz, Ar-H), 6.32 (1H, s, Ar-H), 6.69 (1H, d, <i>J</i> = 8 Hz, Ar-H), 6.96 (1H, s, Ar-H), 7.54 (1H, t, <i>J</i> = 8 Hz, Ar-H), 7.69 (1H, d, <i>J</i> = 8 Hz, Ar-H), 8.15 (1H, d, <i>J</i> = 8 Hz, Ar-H), 8.22 (1H, s, Ar-H)	MALDI-FTMS calcd. For C ₂₇ H ₂₆ N ₃ O ₇ : [M+H] ⁺ 504.176 9. Found 504.176 5
46	White powder, 45.2%	133–135	1.92–2.63 (4H, m, CH ₂ CH ₂), 2.54 (3H, s, NCH ₃), 4.03 (3H, s, OCH ₃), 4.22 (1H, t, NH), 4.33 (2H, d, CH ₂ N), 4.40 (1H, d, <i>J</i> = 4 Hz, CH-N), 5.61 (1H, d, <i>J</i> = 4 Hz, CH-O), 5.94 (2H, s, OCH ₂ O), 6.23 (2H, m, Ar-H), 6.31 (2H, m, Ar-H), 6.70 (1H, d, Ar-H), 7.06 (1H, s, Ar-H), 7.37 (1H, s, Ar-H)	MALDI-FTMS calcd. For C ₂₅ H ₂₅ N ₂ O ₆ : [M+H] ⁺ 449.171 7. Found 449.170 7
47	White powder, 76.0%	67–70	1.95–2.65 (4H, m, CH ₂ CH ₂), 2.54 (3H, s, NCH ₃), 3.95 (2H, t, CH ₂), 4.03 (3H, s, OCH ₃), 4.06 (1H, m, NH), 4.40 (1H, d, <i>J</i> = 4 Hz, CH-N), 5.61 (1H, d, <i>J</i> = 4 Hz, CH-O), 5.93 (2H, s, OCH ₂ O), 6.23 (1H, d, Ar-H), 6.30 (2H, m, Ar-H and CH=), 6.61 (1H, d, CH=), 6.69 (1H, dd, Ar-H), 7.04 (1H, d, Ar-H), 7.24 (1H, m, Ar-H), 7.33 (4H, m, Ar-H)	MALDI-FTMS calcd. For C ₂₉ H ₂₉ N ₂ O ₅ : [M+H] ⁺ 485.208 9. Found 485.207 1
48	White powder, 18.2%	180–183	1.00 (3H, t, CH ₃), 1.64 (2H, m, CH ₂), 1.90–2.70 (4H, m, CH ₂ CH ₂), 2.55 (3H, s, NCH ₃), 3.09 (2H, t, CH ₂), 3.84 (1H, s, NH), 4.01 (3H, s, OCH ₃), 4.42 (1H, s, CH-N), 5.63 (1H, s, CH-O), 5.93 (2H, s, OCH ₂ O), 6.23 (1H, brs, Ar-H), 6.31 (1H, s, Ar-H), 6.64 (1H, d, Ar-H), 6.96 (1H, d, Ar-H)	MALDI-FTMS calcd. For C ₂₃ H ₂₇ N ₂ O ₅ : [M+H] ⁺ 411.192 4. Found 411.191 5

Table 2 Noscapine derivatives (**16–17**, **20–22**) and their cytotoxic activities against HL-60^a. ^aThe cytotoxicity (IC_{50}) is the concentration of compound that reduced the optical density of treated cells by 50% with respect to untreated cells using the MTT assay. Data represent the mean values of three independent determinations. ^b*Erythro* isomer. ^cSeparated by flash chromatography. ^d*Threo* isomer, separated by flash chromatography



Compd.	R ₁	R ₂	R ₃	HL-60 (IC_{50})/ $\mu\text{mol}\cdot\text{L}^{-1}$ ^a
16 ^{b,c}	H	OCH ₃	OCH ₃	28.81
17 ^{c,d}	H	OCH ₃	OCH ₃	36.69
20 ^{b,c}	CN	H	H	48.86
21 ^{b,c}	H	NO ₂	H	14.57
22 ^{b,c}	H	NH ₂	H	9.43
1				19.72
Colchicine				7.45

position of the phenyl ring, was determined to inhibit HL-60 cell line approximately 10-fold more than its parent analogue **23**. A comparable cytotoxic activity was found when replacing the nitro group of **31** by a methoxy group (compound **28**, Table 3). It is noted that the compounds with heterocyclic substitutions

(**32–35**, Table 3) were more potent than most of their phenyl substitution analogs.

6-Amino derivatives **37–48**, compared to the parent analogue **37**, which was devoid of activity, incorporation of nitro group on *meta* or *para* position of the phenyl ring significantly increased the biological activity to the micromolar (**45**, $IC_{50} = 13.06 \mu\text{mol}\cdot\text{L}^{-1}$; **41**, $IC_{50} = 10.71 \mu\text{mol}\cdot\text{L}^{-1}$). Replacement of the nitro group of compound **41** by a methoxy group (compound **38**), abolished the activity. However, when another methoxy group was affiliated to **38** on the *ortho* position of phenyl ring, one of the highest cytotoxic activities was observed (**44**, $IC_{50} = 11.24 \mu\text{mol}\cdot\text{L}^{-1}$). The importance of *ortho*-methoxy group for HL-60 cytotoxic activity was also illustrated by compounds **42** and **43**.

To investigate the precise mechanisms of cell death, the most potent cytotoxic compounds **31** and **44** were chosen to examine the effect on percent G₂/M cells (mitotic index) and sub-G₁ cells (apoptotic index) in HL-60 cells using fluorescence activated cell sorting (FACS) analysis. The flowcytometric evaluation of the cell cycle status was performed as described in the literature^[21]. Figure 2 (A–D) showed the cell cycle profile for the tested compounds included in the course of this study.

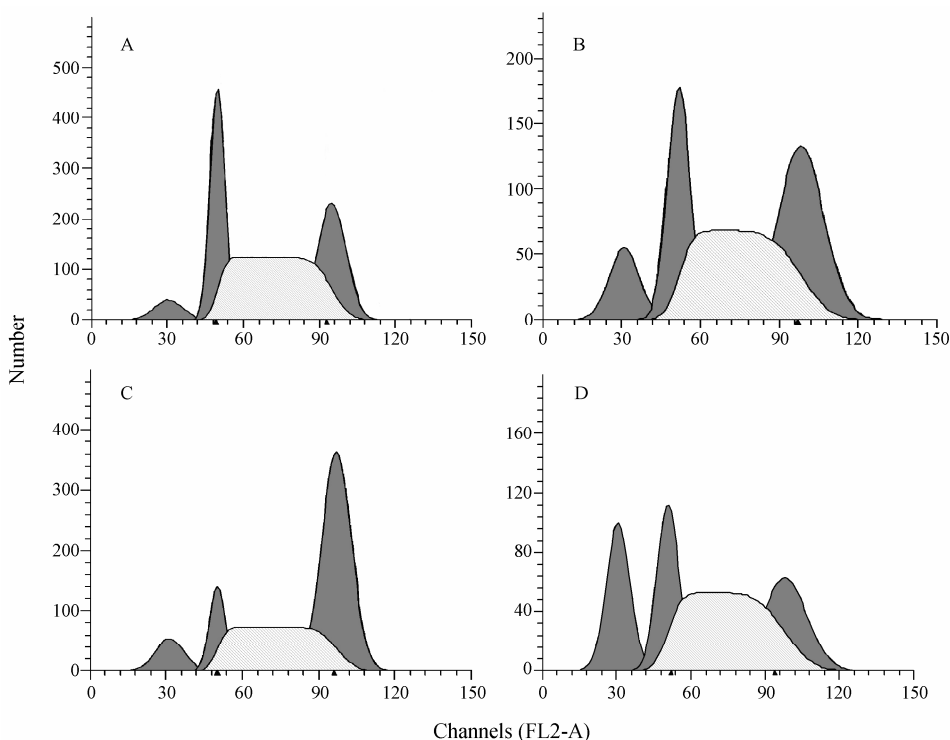


Figure 2 FACS analysis of HL-60 cells treated with agents for 48 h. HL-60 cells treated with (A) DMSO (0.1%), (B) $\alpha(-)$ -noscapine ($50 \mu\text{mol}\cdot\text{L}^{-1}$), (C) compound **31** ($25 \mu\text{mol}\cdot\text{L}^{-1}$), (D) compound **44** ($25 \mu\text{mol}\cdot\text{L}^{-1}$)

Table 3 Noscapine derivatives (**23–48**)^a and their cytotoxic activities against HL-60 and their dissociation constants to tubulin. ^a*erythro* isomer; ^bNT: Not tested

Compd.	R ₄	HL-60 (IC ₅₀)/μmol·L ⁻¹	K _d /μmol·L ⁻¹	Compd.	R ₄	HL-60 (IC ₅₀)/μmol·L ⁻¹	K _d /μmol·L ⁻¹
23		73.44	74.53	37		>100	NT ^b
24		42.31	36.92	38		>100	NT
25		>100	98.01	39		23.42	NT
26		88.63	30.80	40		>100	NT
27		>100	50.34	41		10.71	NT
28		10.01	87.63	42		>100	NT
29		81.31	88.58	43		20.78	NT
30		75.59	70.16	44		11.24	NT
31		6.74	42.14	45		13.06	NT
32		8.02	36.13	46		27.39	NT
33		12.61	130.34	47		>100	NT
34		18.68	42.61	48	CH ₃ CH ₂ -	12.64	NT
35		9.21	1397.9	1		19.72	140.95
36	CH ₃ -	20.99	446.87	Colchicine		7.45	41.22

The distribution of cell population over G₁, S and G₂/M phases of the cell cycle are shown in Table 4. Treatment of HL-60 cells with these compounds for 48 h led to profound perturbations of the cell cycle profile. Our results show that compound **31** induced a massive accumulation of cells in the G₂/M phase, for example, the G₂/M cell population increased from 27% in the control to 54% in HL-60 cells treated with 25 μmol·L⁻¹ compound **31**.

The progressive generation of cells having hypodiploid DNA content indicates apoptotic cells with fragmented DNA. The percent sub-G₁ population has also been plotted for the compounds **31**, **44** and noscapine in Figure 2. It is evident from the

Table 4 Effects on cell cycle distribution

Drug	Conc. /μmol·L ⁻¹	G ₁ /%	S/%	G ₂ /M /%	Apoptosis /%
DMSO	0.1%	36	37	27	4.4
<i>α</i> -(-)-Noscapine, 1	50	25	39	36	8.9
31	25	11	35	54	6.9
44	25	24	48	28	18.7

representation that a 48 h treatment at 25 μmol·L⁻¹ for HL-60 cells, the percentage of sub-G₁ cells is almost similar for compound **31** to noscapine (50 μmol·L⁻¹). However, the sub-G₁ population was much larger for compound **44** at 25 μmol·L⁻¹ than noscapine at 50 μmol·L⁻¹. Thus, we can clearly see compound

44 had shown its deleterious effect on the cell cycle by an increase in the percentage of sub-G₁ cells having hypodiploid DNA content, characteristic of apoptosis.

As noscapine (**1**) is known to induce G₂/M arrest as a result of its binding to tubulin^[6], blocking cell division at mitosis, we further examined the effects of these series of derivatives on tubulin. Tubulin-binding agents typically quench the fluorescence emission spectrum of tubulin in a concentration-dependent manner. This provides the basis for using fluorescence titration method to determine the dissociation constant (K_d) between tubulin and drugs. Fluorescence titration for determining the binding constant was performed as described^[22].

Noscapine and its derivatives **23–36** produced negligible fluorescence emission intensity. Due to the strong fluorescence emission of the 6-alkylamino derivatives **37–48**, the dissociation constants of these compounds were not able to be determined in the assay. The dissociation constants of 6-amido derivatives are summarized in Table 3. The results indicated that twelve out of fourteen 6-amido derivatives showed more potent tubulin binding affinity than noscapine. Generally, compounds with aromatic acyl substitutions showed more appreciable tubulin-binding activity compared to aliphatic acyl substitutions. Compounds with an electron-withdrawing group in the aromatic ring showed a greater affinity to tubulin than those with an electron-donating group. For example, substitution of 4-nitro of **31** ($K_d = 42.12 \mu\text{mol}\cdot\text{L}^{-1}$) with a 4-methoxy group (**28**, $K_d = 87.63 \mu\text{mol}\cdot\text{L}^{-1}$) gave a 2-fold decrease in binding affinity. Different effects were observed by the various heterocyclic acyl substituted 6-amido derivatives **32–35**. Furyl (**32**) molecule had the strongest binding affinity with K_d value of $36.13 \mu\text{mol}\cdot\text{L}^{-1}$, while pyridyl derivative **33** was considerably less active than compound **32**, with K_d value of $130.34 \mu\text{mol}\cdot\text{L}^{-1}$. Surprisingly, indolyl compound **34** showed similar binding affinity to **32**, while indolylpropionyl compound **35** abolished the tubulin-binding activity. Although the exact reason of this decrease was unknown, it could speculate that the indolylpropionyl group with long chain may not accommodate to tubulin well.

The results of the tubulin-binding activity assay were generally coordinated with the MTT assay. The compounds with more potent tubulin-binding activity demonstrated stronger cytotoxic activity against HL-60 cell line, except for compounds **33** and **35**. For example, compound **31** ($K_d = 42.12 \mu\text{mol}\cdot\text{L}^{-1}$) also exhibited

about three times potent than noscapine ($K_d = 140.95 \mu\text{mol}\cdot\text{L}^{-1}$) and equivalent to colchicines ($K_d = 41.22 \mu\text{mol}\cdot\text{L}^{-1}$), which was completely coordinated with MTT assay. It suggests that the antitumor activity of this series of compounds was probably correlated to their effect on tubulin.

Furthermore, the effects of the derivatives on tubulin polymerization were also evaluated. By measuring the changes in the turbidity produced upon tubulin polymerization, the effect of the drugs on the assembly of tubulin subunits into microtubules can be examined. As expected, colchicine strongly inhibited tubulin polymerization at the concentration of $10 \mu\text{mol}\cdot\text{L}^{-1}$ (Figure 3A) in the assay. Noscapine did not inhibit tubulin polymerization at the concentration of $100 \mu\text{mol}\cdot\text{L}^{-1}$ (Figure 3B), which was in agreement with a previous report^[12]. The effects of compound **31** (Figure 3C) and **44** (Figure 3D) on the assembly of tubulin subunits into microtubules were also examined *in vitro* in different concentrations. At the concentrations of 10 and $100 \mu\text{mol}\cdot\text{L}^{-1}$, both compound **31** and **44** inhibited tubulin polymerization, which may suggest that the antitumor activity of compounds were partly attributed to their inhibitory activity on the tubulin polymerization.

3 Conclusions

A novel series of noscapine derivatives were synthesized by a facile and convenient method and their cytotoxic activities were evaluated against HL-60 cell line. Ten of twenty-six screened compounds showed appreciable cytotoxic activities with $\text{IC}_{50} < 20 \mu\text{mol}\cdot\text{L}^{-1}$ against HL-60 cell line. In both of the MTT assay and tubulin binding assay, 3-(4-methoxy-6-methyl-5, 6, 7, 8-tetrahydro-[1, 3]dioxolo[4, 5-g]isoquinolin-5-yl)-6-(4-nitrobenzamido) phthalide **31** had showed about three times more potent than noscapine and equivalent to colchicines, and arrested more cells at the G₂/M phase than noscapine. Moreover, the representative 6-amido derivatives and 6-alkylamino derivatives effectively inhibited tubulin polymerization. Further researches of noscapine analogues involving their antiproliferative activities against other tumor models, structural modification, mechanism study are under progress.

Experimental

1 General methods

Reagents and solvents used were obtained from the supplier without further purification. ¹H NMR spectra and ¹³C NMR spectra were recorded on a Bruker

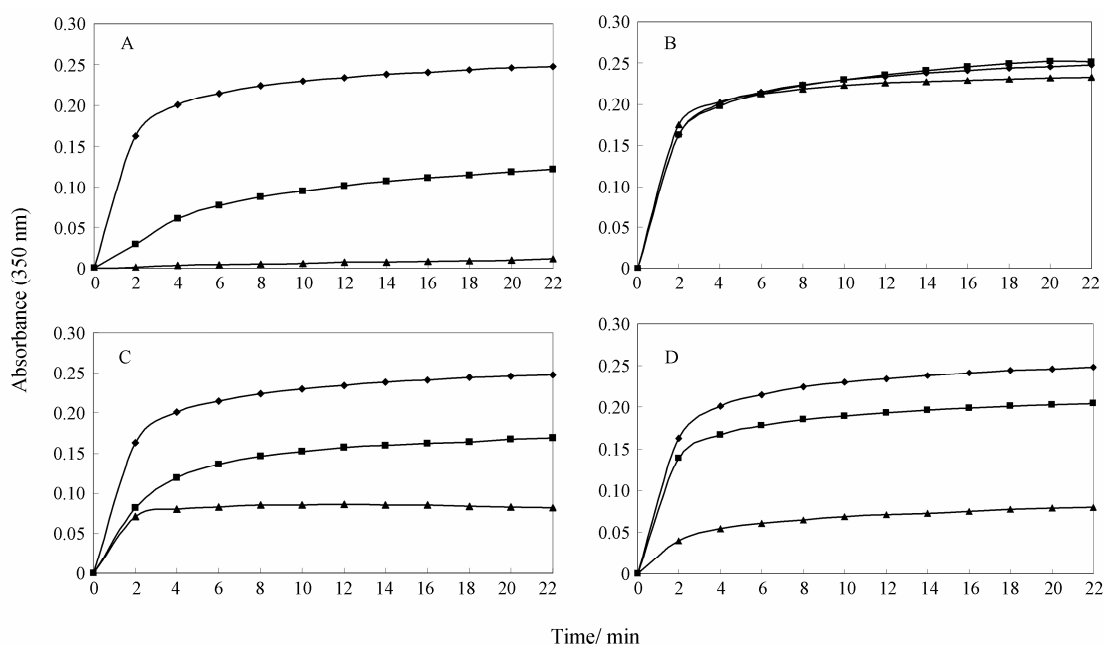


Figure 3 The effects of colchicine, $\alpha(-)$ -noscapine and the derivatives of noscapine on the assembly of tubulin into microtubules. A: Colchicine [control (\blacklozenge), $1 \mu\text{mol}\cdot\text{L}^{-1}$ (\blacksquare) and $10 \mu\text{mol}\cdot\text{L}^{-1}$ (\blacktriangle)]; B: $\alpha(-)$ -Noscapine [control (\blacklozenge), $10 \mu\text{mol}\cdot\text{L}^{-1}$ (\blacksquare) and $100 \mu\text{mol}\cdot\text{L}^{-1}$ (\blacktriangle)]; C: Compound **31** [control (\blacklozenge), $10 \mu\text{mol}\cdot\text{L}^{-1}$ (\blacksquare) and $100 \mu\text{mol}\cdot\text{L}^{-1}$ (\blacktriangle)]; D: Compound **44** [control (\blacklozenge), $10 \mu\text{mol}\cdot\text{L}^{-1}$ (\blacksquare) and $100 \mu\text{mol}\cdot\text{L}^{-1}$ (\blacktriangle)]

INOVA 400 NMR spectrometer and tetramethylsilane (TMS) used as the internal reference in DMSO- d_6 and J values in Hz. Mass spectra, EI and ESI methods, were recorded on Micromass GCT and Agilent Technologies 6130 Quadrupole LC/MS spectrometers, respectively. MALDI-FTMS was recorded on Varian Ionspec 4.7 Telsa mass spectrometer. All melting points are uncorrected and measured in open glass capillaries using SGW X-4 melting point apparatus. Synthetic yields of compounds were not optimized.

2 Chemistry

2.1 Preparation of erythro-3-(4-methoxy-6-methyl-5, 6, 7, 8-tetrahydro-[1, 3]dioxolo [4, 5-g]isoquinolin-5-yl)-6-aminophthalide (22)

To a solution of nitro-substituted compound **21** (0.27 g, 0.678 mmol) in glacial acetic acid (1.08 mL) was quickly added granulated tin (0.14 g, 1.18 mmol) and a solution of hydrated stannous chloride (0.59 g, 2.61 mmol) in concentrated hydrochloride (1.08 mL). After 4 hours the original yellow color had almost disappeared, the mixture was poured into water (30 mL). As soon as 41% potassium hydroxide aqueous solution (12 mL) was added, the aqueous phase was extracted with CHCl_3 and the combined organic layers were washed with brine and then dried over MgSO_4 . The solvent was evaporated under vacuum to give compound **22** in over 90% yield, mp 208–210 °C. ^1H NMR

(DMSO- d_6): 1.88–2.55 (4H, m, CH_2CH_2), 2.41 (3H, s, NCH_3), 3.96 (3H, s, OCH_3), 4.21 (1H, d, $J = 4$ Hz, CH-N), 5.47 (2H, s, NH_2), 5.49 (1H, d, $J = 4$ Hz, CH-O), 6.00 (2H, s, OCH_2O), 6.13 (1H, d, $J = 8$ Hz, Ar-H), 6.47 (1H, s, Ar-H), 6.71 (1H, dd, $J = 2, 8$ Hz, Ar-H), 6.84 (1H, d, $J = 2$ Hz, Ar-H). MS $[\text{M}+\text{H}]^+$ 369.

2.2 Preparation of erythro-6-amido 3-(tetrahydroisoquinolin-5-yl)phthalide derivatives 23-36

2.2.1 erythro-3-(4-methoxy-6-methyl-5, 6, 7, 8-tetrahydro-[1, 3]dioxolo[4, 5-g]isoquinolin-5-yl)-6-benzamidophthalide (23) To a cold mixture of amine **22** (90 mg, 0.245 mmol) and pyridine (0.05 mL) in dry dichloromethane (3 mL) was added a solution of benzoyl chloride (51.3 mg, 0.37 mmol) in dry dichloromethane (2 mL) and the mixture was stirred at room temperature under N_2 for 24 hours. Water (15 mL) was added, and the aqueous phase was extracted with CH_2Cl_2 (15 mL \times 3). The combined organic phase was washed with saturated brines (10 mL), dried over MgSO_4 and concentrated in vacuo. The product was purified by column chromatography (PE–AcOEt– $\text{Et}_3\text{N} = 30 : 5 : 1$) to give **23**.

Compound **24–35** were prepared from **22** and benzoyl chlorides in a manner similar to that described for **23**.

2.2.2 erythro-3-(4-methoxy-6-methyl-5, 6, 7, 8-tetrahydro-[1, 3]dioxolo[4, 5-g]isoquinolin-5-yl)-6-acetylamino-phthalide (36) Amine **22** (100 mg, 0.272

mmol) was dissolved to acetic anhydride (1 mL, 0.6 mmol) and the solution was stirred for 30 min at room temperature. Then the solution was poured into water (30 mL) and rendered alkaline with ammonia. The aqueous phase was extracted with CH_2Cl_2 (12 mL \times 3). The combined organic phase was washed with saturated brines (10 mL), dried over MgSO_4 and concentrated in vacuo to give **36**.

2.3 Preparation of 6-alkylamino 3-(tetrahydroisoquinolin-5-yl)phthalide derivatives **37-48**

erythro-3-(4-methoxy-6-methyl-5, 6, 7, 8-tetrahydro-[1, 3]dioxolo[4, 5-g]isoquinolin-5-yl)-6-benzylaminophthalide (37) Amine **22** (80 mg, 0.217 mmol), benzaldehyde (0.044 mL, 0.435 mol) and glacial acetic acid (0.075 mL) were mixed in dichloromethane (15 mL). Sodium triacetoxyborohydride (129 mg, 0.609 mmol) was added to the above solution and the reaction mixture was stirred at room temperature under N_2 for 24 hours. The solvent was evaporated and methanol (15 mL) was added. Potassium borohydride (50 mg, 0.926 mmol) was added in batches. After 3 h, the solvent was evaporated and saturated aqueous sodium bicarbonate (30 mL) was added. The product was extracted with AcOEt and dried over MgSO_4 . The solvent was evaporated and the residue was purified by column chromatography (CH_2Cl_2 -AcOEt = 40 : 60) to give **37**.

Compound **38-48** were prepared from **22** and benzaldehydes in a manner similar to that described for **37**.

3 Biological

3.1 Cytotoxicity on cancerous cells

HL-60 (Human promyelocytic leukemia cell line) was obtained from the Cell Bank of Chinese Academy of Sciences and cultured in RPMI 1640 (GIBCO Industries Inc.) and 10% (v/v) heat inactivated fetal bovine serum (FBS; GIBCO Industries Inc.) at 37 °C in a humidified atmosphere of 95% air and 5% CO_2 . Cytotoxicity was determined by the MTT [3-(4, 5-dimethylthiazol-2-yl)-2, 5-diphenyl-2H-tetrazolium bromide] assay using a 96-well microtiter plate. The synthetic compound stock solutions were prepared in DMSO. 100 μL cells per well were plated and treatment with these compounds was performed 12 h after plating. Cells were exposed continuously with varying concentrations of drugs and MTT assays were performed at the end of the third day. At the end of the treatments, 100 μL MTT solution (5 $\text{mg}\cdot\text{mL}^{-1}$) per well was added to each culture medium and the cells were incubated for additional 4 hours at 37 °C and

then the medium was removed. The cells were lysed and the formazan crystals were dissolved using 100 μL DMSO. The optical density was determined at a wavelength of 492 nm using 630 nm as reference wavelength using Thermo Multiscan MK5 reader.

3.2 Cell cycle analysis

The flowcytometric evaluation of the cell cycle status was performed as described by Z. Darzynkiewicz et al^[21]. Briefly, HL-60 cells were seeded at 1.5×10^5 cells/mL and incubated at 37 °C in presence of DMSO (the diluent, used as control) or the tested drugs for 43 hours. 9 mL HL-60 cells were centrifuged, washed once with PBS, and fixed in 70% ethanol. Tubes containing the cell pellets were stored at 4 °C for 30 minutes. After this, the cells were centrifuged at 1 500 $\times g$ for 5 minutes and the supernatant was discarded. Cells were then incubated with RNase A (20 $\mu\text{g}\cdot\text{mL}^{-1}$) and propidium iodide (20 $\mu\text{g}\cdot\text{mL}^{-1}$) in PBS for 30 minutes, separately. The samples were analyzed on a Becton Dickinson FACS Calibur flowcytometer.

3.3 Tubulin binding assay

Fluorescence titration for determining the binding constant was performed as described^[21, 22]. In brief, noscapine and 6-amido 3-(tetrahydroisoquinolin-5-yl)phthalide derivatives (0-100 $\mu\text{mol}\cdot\text{L}^{-1}$) were incubated with 2 $\mu\text{mol}\cdot\text{L}^{-1}$ tubulin in PM buffer (100 $\text{mmol}\cdot\text{L}^{-1}$ PIPES, 2 $\text{mmol}\cdot\text{L}^{-1}$ EGTA, 1 $\text{mmol}\cdot\text{L}^{-1}$ MgSO_4 , 2 $\text{mmol}\cdot\text{L}^{-1}$ DTE) at 37 °C for 45 min. The fluorescence emission spectra were recorded using Varian Cary Eclipse scanning fluorescence spectrophotometer equipped with a Xenon flash lamp and the excitation wavelength was 295 nm.

The values of dissociation constant were determined according to the formula: $1/B = K_d / [\text{free ligand}] + 1$, where B is the fractional occupancy and [free ligand] is the concentration of candidate. The fractional occupancy (B) was obtained by the formula: $B = \Delta F / \Delta F_{\text{max}}$, where ΔF is the change in fluorescence intensity when tubulin and its ligand are in equilibrium and ΔF_{max} is the value of maximum fluorescence change when tubulin is completely bound with its ligand. ΔF_{max} was calculated by plotting $1/\Delta F$ versus $1/[\text{free ligand}]$.

3.4 Tubulin polymerization assay

Spectrophotometer cuvettes (1-cm path length) held a solution consisting of 10 $\mu\text{mol}\cdot\text{L}^{-1}$ tubulin, PM buffer (100 $\text{mmol}\cdot\text{L}^{-1}$ PIPES, 2 $\text{mmol}\cdot\text{L}^{-1}$ EGTA, 1 $\text{mmol}\cdot\text{L}^{-1}$ MgSO_4 , 2 $\text{mmol}\cdot\text{L}^{-1}$ DTE) and 1 or 10 $\mu\text{mol}\cdot\text{L}^{-1}$ colchicine, 10 or 100 $\mu\text{mol}\cdot\text{L}^{-1}$ noscapine, different concentrations of compound **31** or compound

44. The solvent DMSO was used as control. Cuvettes were kept for 15 min at 37 °C before quickly cooled to 0 °C and then left at 0 °C for another 10 min. Then, add GTP to a final concentration of 1 mmol·L⁻¹. The solution was monitored by measuring the changes in absorbance at 350 nm by HITACHI U2910 spectrophotometer equipped with a constant temperature device at 2 min intervals with PM buffer as reference.

References

- [1] Verma AK, Bansal S, Singh J, et al. Synthesis and *in vitro* cytotoxicity of haloderivatives of noscapine [J]. *Bioorg Med Chem*, 2006, 14: 6733–6736.
- [2] Van Tellingen O, Sips JHM, Beijnen JH, et al. Pharmacology, bio-analysis and pharmacokinetics of the vinca alkaloids and semi-synthetic derivatives [J]. *Anticancer Res*, 1992, 12: 1699–1715.
- [3] Liu M, Luo XJ, Liao F, et al. Noscapine induces mitochondria-mediated apoptosis in gastric cancer cells *in vitro* and *in vivo* [J]. *Cancer Chemother Pharmacol*, 2011, 67: 605–612.
- [4] Niyati J, Heeyeon C, Shering T, et al. Noscapine inhibits tumor growth in TMZ-resistant gliomas [J]. *Cancer Lett*, 2011, 312: 245–252.
- [5] David GIK. Tubulin-interactive natural products as anticancer agents [J]. *J Nat Prod*, 2009, 72: 507–515.
- [6] Landen JW, Lang R, McMahon SJ, et al. Noscapine alters microtubule dynamics in living cells and inhibits the progression of melanoma [J]. *Cancer Res*, 2002, 62: 4109–4114.
- [7] Aneja R, Dhiman N, Idnani J, et al. Preclinical pharmacokinetics and bioavailability of noscapine, a tubulin-binding anticancer agent [J]. *Cancer Chemother Pharmacol*, 2007, 60: 831–839.
- [8] Aneja R, Ghaleb AM, Zhou J, et al. p53 and p21 determine the sensitivity of noscapine-induced apoptosis in colon cancer cells [J]. *Cancer Res*, 2007, 67: 3862–3870.
- [9] Aneja R, Vangapandu SN, Lopus M, et al. Synthesis of microtubule-interfering halogenated noscapine analogs that perturb mitosis in cancer cells followed by cell death [J]. *Biochem Pharmacol*, 2006, 72: 415–426.
- [10] Aneja R, Zhou J, Zhou BF, et al. Treatment of hormone-refractory breast cancer: apoptosis and regression of human tumors implanted in mice [J]. *Mol Cancer Ther*, 2006, 5: 2366–2377.
- [11] Bokyoung S, Kwang SA, Bharat BA. Noscapine, a benzyloisoquinoline alkaloid, sensitizes leukemic cells to chemotherapeutic agents and cytokines by modulating the NF- κ B signaling pathway [J]. *Cancer Res*, 2010, 70: 3259–3268.
- [12] Zhou J, Panda D, Landen JW, et al. Minor alteration of microtubule dynamics causes loss of tension across kinetochore pairs and activates the spindle checkpoint [J]. *J Biol Chem*, 2002, 277: 17200–17208.
- [13] Aneja R, Vangapandu SN, Joshi HC. Synthesis and biological evaluation of a cyclic ether fluorinated noscapine analog [J]. *Bioorg Med Chem*, 2006, 14: 8352–8358.
- [14] Anderson JT, Ting AE, Boozer S, et al. Identification of novel and improved antimetabolic agents derived from noscapine [J]. *J Med Chem*, 2005, 48: 7096–7098.
- [15] Alexander RS. Pyrogallol 1-monomethyl ether [J]. *Org Syn*, 1946, 26: 90–92.
- [16] Shirasaka T, Takuma Y, Shimpuku T, et al. Practical synthesis of 5, 6, 7, 8-tetrahydro-4-methoxy-6-methyl-1, 3-dioxolo[4, 5-g]isoquinolin-5-ol (cotarnine) [J]. *J Org Chem*, 1990, 55: 3767–3771.
- [17] Shono T, Hamaguchi H, Sasaki M, et al. Novel zinc-promoted alkylation of iminium salts. New synthesis of benzyloisoquinoline, phthalidylisoquinoline, and protoberberine alkaloids and related compounds [J]. *J Org Chem*, 1983, 48: 1621–1628.
- [18] Hope E, Robinson R. Synthetic experiments in the group of the iso-quinoline alkaloids. I. Anhydrocotarninephthalide [J]. *J Chem Soc*, 1911, 99: 1153–1169.
- [19] Kinuko I, Miyoko K, Makiko S, et al. Conformations of phthalideisoquinoline salts and *N*-oxides [J]. *J Nat Prod*, 1987, 50: 1083–1088.
- [20] Scudiero DA, Shoemaker RH, Paul KD, et al. Evaluation of a soluble tetrazolium/formazan assay for cell growth and drug sensitivity in culture using human and other tumor cell lines [J]. *Cancer Res*, 1988, 48: 4827–4833.
- [21] Darzynkiewicz Z, Bruno S, Del Bino G, et al. Features of apoptotic cells measured by flowcytometry [J]. *Cytometry*, 1992, 13: 795–808.
- [22] Zhou J, Gupta K, Aggarwal S, et al. Brominated derivatives of noscapine are potent microtubule-interfering agents that perturb mitosis and inhibit cell proliferation [J]. *Mol Pharmacol*, 2003, 63: 799–807.